Biochemical and Biophysical Research Communications 463 (2015) 193–199

Contents lists available at ScienceDirect

Biochemical and Biophysical Research Communications

journal homepage: www.elsevier.com/locate/ybbrc

Changes in white and brown adipose tissue microRNA expression in cold-induced mice

Cong Tao [a, b], Shujuan Huang [b], Yajun Wang [b], Gang Wei [c], Yang Zhang [b], Desheng Qi [a, *], Yanfang Wang [b, **], Kui Li [b]

[a] Department of Animal Nutrition and Feed Science, College of Animal Science and Technology, Huazhong Agricultural University, Wuhan, Hubei 430070, China
[b] State Key Laboratory of Animal Nutrition, Institute of Animal Science, Chinese Academy of Agriculture Sciences, Beijing 100193, China
[c] Key Laboratory of Animal Ecology and Conservation Biology, Institute of Zoology, Chinese Academy of Sciences, Beijing 100101, China

ARTICLE INFO

Article history:
Received 28 April 2015
Available online 15 May 2015

Keywords:
microRNAs
Brown adipose tissue
Inguinal white adipose tissue
Cold
Uncoupling protein 1

ABSTRACT

There are two classic adipose tissues in mammals, white adipose tissue (WAT) and brown adipose tissue (BAT). It has been well known that browning of WAT can be induced by cold exposure. In this study, to identify the novel cold responsive key miRNAs that are involved in browning, mice were housed at 6 °C for 10 days, and deep sequencing of the miRNAs of WAT and BAT was performed. Our data showed that WAT and BAT displayed distinct expression profiles due to their different locations, morphology and biological function. A total of 27 BAT and 29 WAT differentially expressed (DE) miRNAs were identified in response to cold stimulation, respectively (fold change >2 and false discovery rate (FDR) <0.05), of which, 9 were overlapped in both adipose tissues. Furthermore, the potential target genes of the DE miRNAs from BAT and WAT were predicted computationally, and the KEGG pathway analysis revealed the enrichment pathways in cold stimulated adipose tissues. The expression pattern of miR-144-3p/Bmpr1b/Phlda1 and miR-146a-5p/Sphk2 were further measured by qPCR. Finally, we found that miR-146a-5p was significantly induced during the primary adipogenesis caused by BAT differentiation, whereas miR-144-3p was decreased. Our study identifies for the first time the novel miRNAs involved in browning of WAT by sequencing and expands the therapeutic approaches for combating metabolic diseases.

1. Introduction

There are two functionally distinct adipose tissues in mammals, white adipose tissue (WAT) and brown adipose tissue (BAT). WAT has the unique function of storing triglycerides (TGs). In contrast, BAT is found in the interscapular region in rodents and combusts excess energy through mitochondrial energy uncoupling mediated by uncoupling protein 1 (Ucp1) in nonshivering thermogenesis. In addition to classical brown and white adipocytes, inducible UCP1-expressing adipocytes have been identified in WAT and are designated brite (brown-in-white) or beige adipocytes [1]. Cold-induced brown adipocytes were found in the WAT of adult humans recently, which generated considerable optimism that beige adipocytes would offer a therapeutic target to combat obesity and metabolic disease [2]. Therefore, better understanding the browning of WAT at the molecular level has become an area of intense investigation.

Substantial research has been performed on the adipose tissue response to cold stimulation in different species and genomewide screening provides the valuable information about the genes and pathways involved in this important biological process [3,4]. The key molecules involved in the browning of WAT have been illustrated; for example, the transcription factors, including PRDM16, PPARγ and C/EBPα, were proven to play the important role in browning [5]. The subcutaneous adipose depot is an most reactive to acquire BAT characteristics, whereas visceral depots are much less responsive [6,7].

MiRNAs have been reported to control key processes in fat metabolism such as adipocyte fat deposition, differentiation and brown adipogenesis [8,9]. Dicer and Dgcr8, the key regulators of

* Corresponding author. College of Animal Science and Technology, Huazhong Agricultural University, No. 1 Shizishan Street, Hongshan District, Wuhan, Hubei, China.
** Corresponding author. State Key Laboratory of Animal Nutrition, Institute of Animal Science, Chinese Academy of Agriculture Sciences, No. 2 Yuanmingyuan West Road, Beijing, China.
E-mail addresses: qds@mail.hzau.edu.cn (D. Qi), wangyanfang@caas.cn (Y. Wang).

http://dx.doi.org/10.1016/j.bbrc.2015.05.014
0006-291X/

microRNA biogenesis, are required for the formation of white and brown adipose tissue, respectively [10,11]. Recently, more and more related studies have focused on the browning of white adipose tissues and brown adipogenesis in adaptive thermogenesis [8,11]. For example, miR-133 has been demonstrated to play a critical role in brown fat differentiation through its target, Prdm16 [12]. A recent study revealed the effect of miR-155 in controlling the development of brown and beige fat cells, through its targeting of C/EBPβ [13]. In addition, it has been reported that overexpression of miR-196a induces the browning of inguinal-WAT (Ing-WAT) in mice [14]. However, to date, miRNA profile-based studies to investigate the murine BAT and WAT response to prolonged cold stimulation have not been reported.

In this study, we analyzed the miRNA profiles in BAT and Ing-WAT upon prolonged cold exposure and identified the novel miRNAs that are involved in the cold-induced activation of BAT and Ing-WAT. The target genes of the DE miRNAs were predicted and the involved pathways were characterized. Our studies should expand the elucidation of cold responsive miRNA in adipose tissue.

2. Materials and methods

2.1. Animal experiments

C57BL/6 male mice at 8 weeks of age housed under standard conditions with ad libitum access to food were randomly divided into two groups. One group of mice was placed at 28 °C and the other group was placed at 6 °C for 10 days. Animals were individually housed with a 12:12-h light–dark cycle and free access to standard chow diet and water. Adipose tissues, including interscapular BAT, Ing-WAT and gonadal WAT (Gon-WAT), were taken from each animal and immediately frozen in liquid nitrogen followed by storage at −80 °C prior to analysis. All experiments involving mice were approved by the Institutional Animal Care Research Advisory Committee of the CAAS.

2.2. Small RNA library construction and sequencing

Briefly, total RNA was isolated using TRIzol reagent (Invitrogen). The quality and integrity of the prepared RNA samples were confirmed using an Agilent 2100 bioanalyzer (Agilent Technologies). Approximately 1 mg of total RNA was used to prepare the small RNA library according to the protocol of TruSeq Small RNA Sample Prep Kits (Illumina). Approximately 16–32 nt RNA fragments were excised and purified from a PAGE gel, and adaptors were ligated to their 5′ and 3′ ends using T4 RNA ligase. RT-qPCR was performed for 17 cycles using adaptor primers and the DNA fragments were subsequently isolated from agarose gel. Single-end sequencing (50 bp) was performed on an Illumina Hiseq 2500 to produce 50 bp single reads at Berry Genomics (Beijing, China) following the recommended protocol.

2.3. Analysis of the deep sequencing data

Primary data analysis: sequences were obtained using Illumina HiSeq. Reads were mapped against Illumina adaptor sequences using blat 17, and the 30 adaptors were subsequently clipped from the reads using NGS QC Toolkit (v2.3) [15]. The reads were then filtered for low complexity regions, resulting in the inclusion of more than 60% of reads on average for each sample. We then used Burrows-Wheeler alignment (BWA) to align the reads to the miRBase version 21 mouse database. The sequences matching known miRNAs were clustered and counted; the PMMR (sequences per million mapped reads) method was introduced to display the miRNA expression. The significantly DE microRNAs were screened with the criteria of fold change >2, P-value < 0.05 and FDR < 0.05.

MiRNA target prediction was performed using scripts from Targetscan 6.2 and miRNA-mRNA interaction networks were visualized using Cytoscape. Pathway annotation of the miRNA targets was performing by the GenCodis 2.0 software [16]. The target genes were mapped to the GO annotation dataset, and the enriched p values were calculated using the hypergeometric test.

2.4. Real-time PCR analysis

Total RNA (0.5 μg for miRNA and 2 μg for mRNA) was reverse-transcribed using the First Strand cDNA Synthesis Kit (Thermo Scientific) [17]. RT-qPCR was performed using SYBR Green master mix (Applied Biosystems) and the 7500 Fast Real Time PCR system (Applied Biosystems). The expression levels were normalized to those of the housekeeping gene 18s. RT-qPCR of the miRNAs was performed using specific stem-loop primers and U6 snRNA was used as an internal reference [18]. The experiment was conducted in triplicate. The primers used for qPCR are shown in Supplementary Table 3. Relative gene expression was calculated using the comparative cycle threshold ($2^{-\Delta\Delta Ct}$) method.

2.5. Western blotting

For Western blot analysis, the tissues were lysed in T-PER Tissue Protein Extraction Reagent (Thermo-Fisher) in the presence of a protease inhibitor cocktail (Roche). The lysates and protein markers (Fermentas) were resolved via SDS-PAGE, transferred to PVDF membranes (Millipore), and probed using anti-UCP1 (1:1000, cat. no. 10983, Abcam) and anti-β-actin antibodies (1:2000, cat. no. 12620, CST). The immunoreactive bands were detected using Pierce ECL Western Blotting Substrate (Thermo).

2.6. Histological studies

Tissues were dissected and fixed in 4% paraformaldehyde overnight and rinsed with phosphate-buffered saline before embedding in paraffin. Paraffin-embedded BAT and Ing-WAT were sectioned at a thickness of 5 μm and stained with hematoxylin and eosin (H&E) [19]. For immunohistochemistry analysis, paraffin-embedded dewaxed sections were incubated with anti-UCP1 (1:500, cat. no. 10983; Abcam) according to the avidin-biotin complex method.

2.7. Cell culture

The primary culture of brown preadipocyte cell lines from new born pups was performed as previously described [20].

2.8. Statistical analysis

The data are presented as the means ± SEM. The values were analyzed via two-tailed independent sample Student's t tests, as appropriate, using GraphPad Prism version 6. A value of $P < 0.05$ was considered to be significant.

3. Results

3.1. Cold-activated brown and white adipose tissue in mice

To explore the adipose miRNAs changes in expression and to identify the key miRNAs in the browning of WAT during cold exposure, male mice at 8 weeks of age were housed in 28 °C and 6 °C for 10 days and the adipose depots were analyzed. Compared

to BAT, the Ing-WAT exhibited dramatic changes upon cold exposure, with a browning process and less fat depots. Fig. 1A shows the representative Ing-WAT and brown fat from mice exposed at 28 °C and 6 °C. The normalized weight of Ing-WAT and Gon-WAT were significant lower in mice at 6 °C, compared to those from 28 °C, whereas the BAT did not exhibit weight changes during cold exposure (Fig. 1B). H&E staining confirmed the browning of Ing-WAT (Fig. 1C).

We also detected the expression level of Ucp1, a classic cold-induced gene in BAT and Ing-WAT, at 28 °C and 6 °C. As shown in Fig. 1D, *Ucp1* mRNA was significantly up-regulated by approximately 3.5-fold in the BAT and 143-fold in the Ing-WAT during prolonged cold treatment (Fig. 1D). Increase of UCP1 in BAT and Ing-WAT were further confirmed at the protein level by immunoblotting (Fig. 1E) and immunofluorecence (Fig. 1F).

3.2. Intrinsic differences between the miRNA profiles of BAT and WAT

The differences between the miRNAs profiles of BAT and WAT were determined by comparison of the miRNAs expression levels between BAT and Ing-WAT at 28 °C. Based on the criteria of fold change >2 and FDR <0.05, 86 miRNAs were identified to be differentially expressed between BAT and WAT, of which 47 were up-regulated and 39 were down-regulated in BAT (Supplementary Table 1). Among the 47 up-regulated miRNAs, some miRNAs showed high expression levels in BAT, whereas they were absent in WAT, such as miR-499-5p, miR-883a-5p, miR-107-5p and miR-6481. Similarly, among the 39 down-regulated miRNAs, some were enriched in WAT and absent in BAT, for example, miR-196a-5p, miR-196b-5p, miR-196a-2-3p and miR-20b-5p. Our data revealed the distinct expression difference between BAT and Ing-WAT.

3.3. DE miRNAs in WAT and BAT during cold exposure

To elucidate the DE miRNAs in adipose tissue upon prolonged cold exposure, comparisons of mapped miRNAs in BAT and Ing-WAT from mice housed at 28 °C and 6 °C were conducted. Based on the criteria of fold change >2 and FDR <0.05, a total of 27 DE miRNAs were screened in cold-stimulated BAT, of which 17 were up-regulated and 10 were down-regulated. Similarly, compared to Ing-WAT from 28 °C, the miRNA response to cold exposure identified 29 DE miRNAs with the same criteria, of which 7 miRNAs were up-regulated and 22 miRNAs were down-regulated (Fig. 2A and B). Of these cold responsive DE miRNAs, nine were found to be overlapped in both BAT and Ing-WAT. They exhibited the same expression patterns, with miR-144-3p, miR-203-5p, miR-6538 and miR-3076-5p being induced and miR-146a-5p, miR-146b-5p, miR-150-3p, miR-342-3p and miR-342-5p being repressed in both adipose tissues upon cold exposure (Fig. 2). Tables 1 and 2 list the 14 DE miRNAs with high abundance in BAT and Ing-WAT.

3.4. Target prediction and pathway enrichment analysis of cold-responsive miRNAs

MiRNAs exert their biological function through their targets genes. The putative target genes of DE miRNAs from BAT and Ing-WAT were predicted by TargetScan. A total of 1765 putative targets were predicted by 27 DE miRNAs from cold-induced BAT, whereas 29 DE miRNAs from Ing-WAT predicted 2856 potential target genes.

To elucidate the pathways and the biological processes that DE miRNAs are involved in, 1765 and 2856 putative targets of DE miRNAs from cold-induced BAT and Ing-WAT were subjected to KEGG pathway analysis. The significantly enriched pathways were analyzed by Fisher's exact test (FDR < 0.001). Fig. 3 shows the top

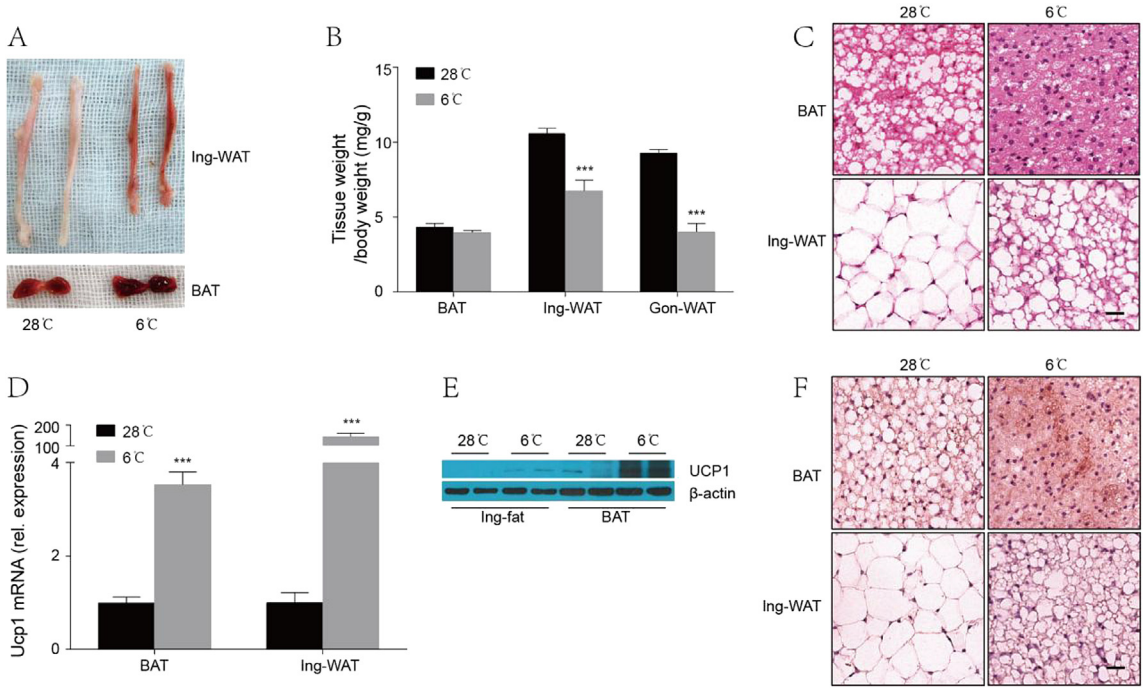

Fig. 1. Browning of white adipose tissue and induction of BAT activation after cold exposure. (A) BAT, and Ing-WAT were isolated at 28 °C and 6 °C. (B) Weights of BAT, ing-WAT and Gon-WAT relative to body weight of mice exposed at 28 °C and 6 °C for 10 days, n = 6. H&E staining (C) and UCP1 immunohistochemistry (F) of BAT and ing-WAT from mice exposed at 28 °C and 6 °C. (D, E) Ucp1 expression in BAT and ing-WAT from mice exposed at 28 °C and 6 °C detected by RT-qPCR (n = 6) and western blot. All of the results are presented as the mean ± SEM; *P < 0.05, **P < 0.01 and ***P < 0.001.

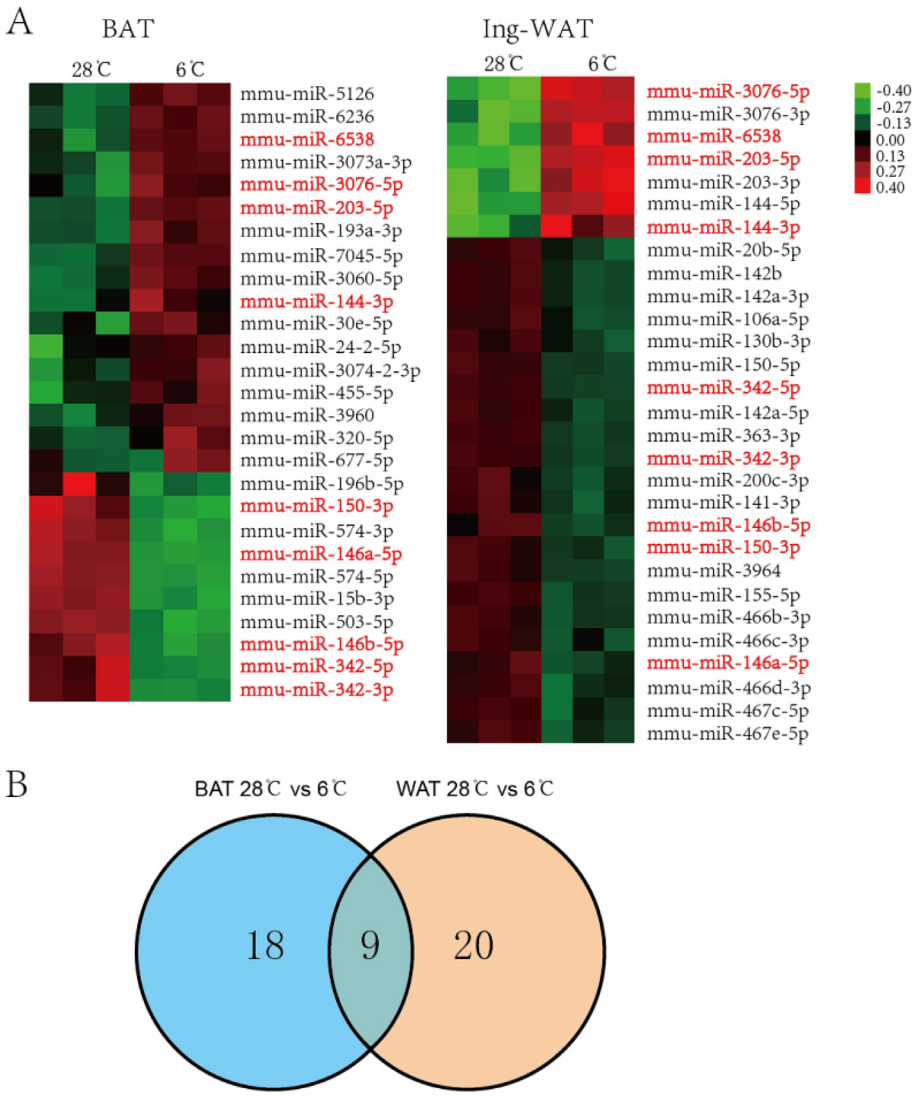

Fig. 2. DE miRNAs in BAT and ing-WAT during cold exposure. (A) Heat maps were built by hierarchical clustering of the DE miRNAs. Red highlighted represents the overlap miRNAs in both BAT and Ing-WAT. (B)Venn diagrams show the overlap of significantly DE miRNAs (fold change >2 and FDR <0.05) in mice exposed at 28 °C and 6 °C. (For interpretation of the references to colour in this figure legend, the reader is referred to the web version of this article.)

15 significantly enriched pathways in cold-induced BAT and Ing-WAT (Fig. 3). Our data indicated that most pathways (10 of 15) were enriched in both BAT and Ing-WAT and were involved in response to prolonged cold stimulation (Fig. 3). Five pathways known to be involved in cancer, including Wnt signaling, Ras signaling, prostate cancer, HTLV-I infection and Melanoma pathways, were only found in cold-induced BAT (Fig. 3A), whereas Axon signaling, endocytosis, ErbB signaling, chronic myeloid leukemia and TGF-beta signaling pathways were only significantly enriched in cold-stimulated Ing-WAT (Fig. 3B).

Table 1
Summary of the differentially expressed miRNAs with high abundance in BAT.

MiRNAs	Count in BH[a]	Count in BL[a]	Fold change	P-value	FDR
miR-144-3p	14920	42538	2.85	6.41E-04	2.36E-02
miR-146a-5p	1981	432	−4.59	7.79E-07	7.54E-05
miR-146b-5p	2379	845	−2.82	4.36E-04	1.87E-02
miR-193a-3p	1375	4399	3.20	1.32E-04	6.79E-03
miR-203-5p	468	4963	10.59	2.49E-13	7.63E-11
miR-3060-5p	204	6935	33.94	1.67E-11	3.85E-09
miR-30e-5p	32728	84043	2.57	1.56E-03	4.47E-02
miR-320-5p	145	843	5.82	2.87E-05	2.03E-03
miR-342-3p	5325	2092	−2.54	1.36E-03	4.03E-02
miR-3960	147	1009	6.85	3.22E-08	4.55E-06
miR-455-5p	719	1955	2.72	1.11E-03	3.46E-02
miR-503-5p	994	373	−2.66	1.15E-03	3.47E-02
miR-5126	35111	494923	14.10	1.44E-14	5.30E-12
miR-574-3p	1475	507	−2.91	4.51E-04	1.89E-02

[a] BH is BAT at 28 °C, BL is BAT at 6 °C.

As described above, 9 DE miRNAs overlapped in cold-stimulated BAT and Ing-WAT, and 5 of them (miR-144-3p, miR-146a-5p, miR-146b-5p, miR-203-3p and miR-342-3p) exhibited high expression levels in BAT and/or Ing-WAT. We are particularly interested in the pathways these miRNAs are involved, and the KEGG pathway analysis of their potential targets was performed. The significant pathways and the representative targets from these miRNAs are listed in Supplementary Table 2.

3.5. miRNAs-mRNAs expression validation

To confirm the DE miRNAs from our sequencing analysis, miR-144-3p and miR-146a-5p, which are cold-responsive miRNAs in both BAT and WAT, were selected for further confirmation. Their potential targets, Bmpr1b and Phlda1 for miR-144-3p

Table 2
Summary of the differentially expressed miRNAs with high abundance in Ing-fat.

MiRNAs	Count in WH[a]	Count in WL[a]	Fold change	P-value	FDR
miR-142a-3p	122361	23728	−5.16	4.64E-08	1.08E-05
miR-142a-5p	49821	9404	−5.30	4.58E-08	1.08E-05
miR-142b	123205	23875	−5.16	4.56E-08	1.08E-05
miR-144-3p	4126	13503	3.27	1.10E-04	5.67E-03
miR-146a-5p	8197	1813	−4.52	4.89E-07	6.80E-05
miR-146b-5p	6799	2012	−3.38	4.42E-05	2.74E-03
miR-150-3p	1000	154	−6.51	1.44E-08	5.36E-06
miR-150-5p	51548	10325	−4.99	9.09E-08	1.88E-05
miR-155-5p	8379	1991	−4.21	1.79E-06	1.98E-04
miR-200c-3p	713	171	−4.17	4.20E-06	3.55E-04
miR-203-3p	10244	31252	3.05	1.30E-04	6.38E-03
miR-203-5p	364	5425	14.89	1.21E-16	2.25E-13
miR-20b-5p	1005	169	−5.95	8.00E-09	4.96E-06
miR-342-3p	13222	3607	−3.67	1.22E-05	9.08E-04

[a] WH is WAT at 28 °C, WL is WAT at 6 °C.

and Sphk2 for miR-146a-5p, were chosen for *miRNAs-mRNAs* interaction validation by qPCR because these genes have been reported to be involved in fat metabolism [21–23]. As shown in Fig. 4, the expression level of miR-144-3p was significantly increased approximately three-fold in both BAT (Fig. 4A) and WAT (Fig. 4C), which is consistent with our sequencing data results. As expected, its putative target, Phlda1, was significantly down-regulated upon cold stimulation in both BAT (Fig. 4A) and WAT (Fig. 4C). However, the significant down-regulation of Bmpr1b, another potential target of miR-144-3p, was only observed in cold-induced BAT (Fig. 4A and C). Similarly, in agreement with our sequencing results, miR-146a-5p was repressed significantly in both cold-stimulated BAT and Ing-WAT, however, its putative target, Sphk2, only showed up-regulation in BAT (Fig. 4B and D).

3.6. Expression of miR-144-3p and miR-146a-5p in BAT differentiation

To further investigate the function of miR-144-3p and miR-146a-5p in BAT differentiation, the brown adipocytes from new born pups were primarily cultured, and the expression levels of miR-144-3p and miR-146a-5p were measured during the course of BAT differentiation. As shown in Fig. 4E, miR-146a-5p showed significant up-regulation during adipogenesis (Fig. 4E) along with the expression of adipogenic markers, such as PPARγ and C/EBPα (Fig. 4F). However, a slight down-regulation expression trend was observed in miR-144-3p during adipogenesis due to BAT differentiation (Fig. 4E).

4. Discussion

In this study, deep sequencing analysis and qPCR were used to investigate the miRNA expression profiles of mouse BAT and WAT in response to cold exposure for 10 days. Such a prolonged cold stimulation has been reported previously to result in activation of adipose tissue [3,4,6]. Our data revealed the distinct miRNA profiles in mouse BAT and WAT and identified several key microRNAs that are important for acquiring brown fat features in WAT depots and brown adipogenesis. The effect of prolonged cold stimulation was validated by significantly induced expression of UCP1 in the BAT and Ing-WAT depots.

We identified a set of miRNAs, that can be triggered by cold exposure in both BAT and WAT. We found that miR-203-5p was significantly up-regulated in adipose tissues upon cold stimulation, which was consistent with the previous observation that miR-203 was induced during brown adipocyte differentiation and functioned as a regulator of brown adipocyte development [11]. There is evidence that miR-193b/miR-365 clusters, brown fat enriched miRNAs, regulate brown fat differentiation not only in the differentiation of primary preadipocyte, but also by inducing myoblasts to differentiate into brown adipocytes via their target genes [24]. Our observation of significant up-regulation of miR-193a in cold exposure BAT suggests that miR-193a may also exert its regulatory function in BAT development. However, miR-155, which was found as a key regulator controlling the development of brown and beige fat cells through C/EBPβ [13], did not show changes in its expression level in the adipose tissue that we tested. The reason for this might be that cold-inducible WAT browning is a dynamic process and the

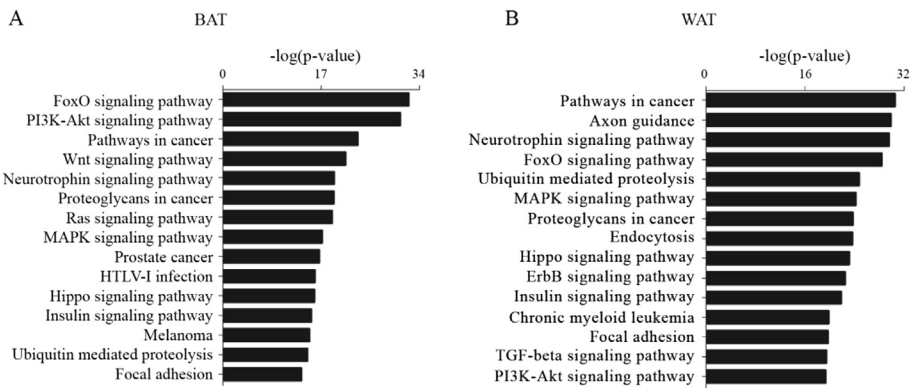

Fig. 3. Enriched KEGG pathways of potential target genes in BAT (A) and Ing-WAT (B). The bars represent significance.

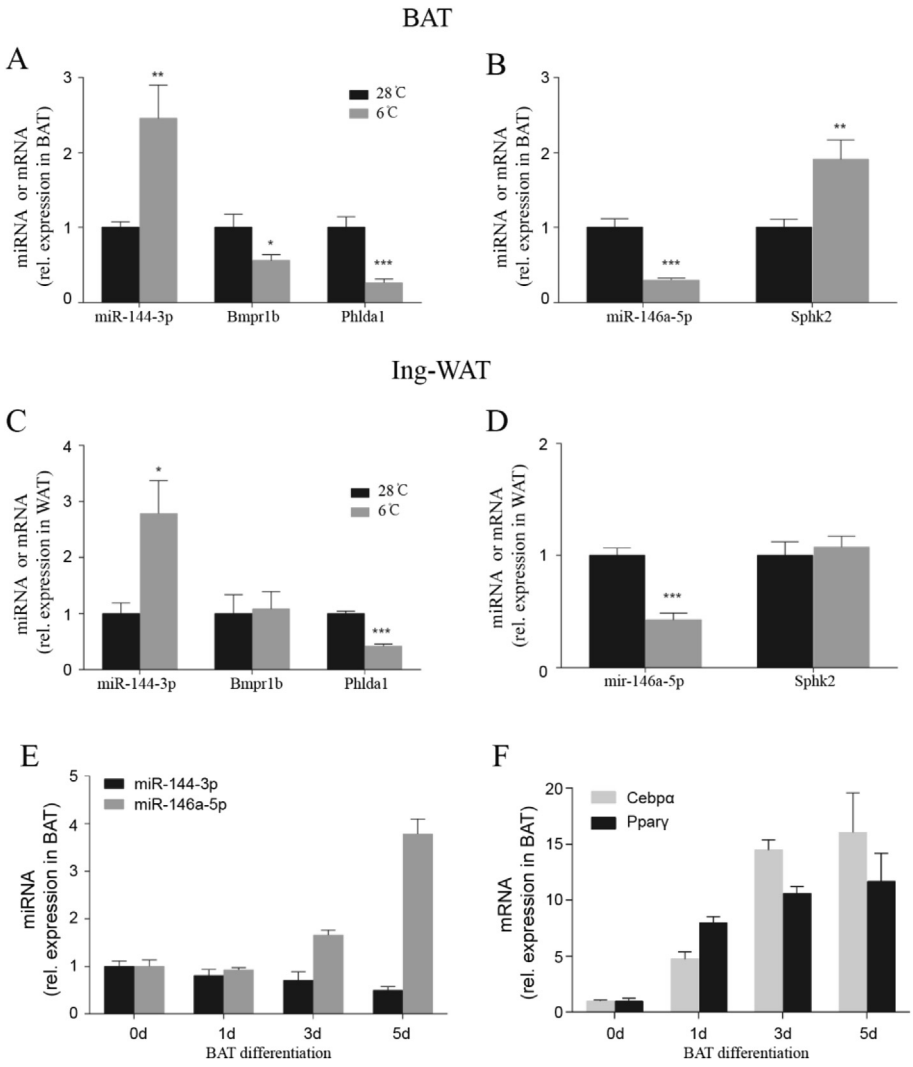

Fig. 4. Expression pattern of selected miRNA-mRNA in adipose tissues at 28 °C and 6 °C and expression levels of miR-144-3p and miR-146a-5p during BAT differentiation. (A–D) Relative expression of miR-144-3p and miR-146a-5p and their putative target genes in BAT (A, B) and Ing-WAT (C, D) of mice exposed at 28 °C and 6 °C, n = 6. (E) Relative expression of miR-144-3p and miR-146a-5p in primary brown adipocytes during differentiation (n = 3). (F) Expression levels of the differentiation markers *Cebpα* and *Pparγ* (n = 3). The results are presented as the mean ± SEM; *P < 0.05, **P < 0.01 and ***P < 0.001.

expression of miR-155 was only measured at the end point of cold treatment.

The potential targets of the five overlapped DE miRNAs were subjected to KEGG analysis, and we are particularly interested in miR-144-3p and miR-146a-5p because these two miRNAs have been implicated in metabolic syndromes in mouse and/or humans [25,26]. Our data showed that miR-144-3p is involved in the adipocytokine signaling pathway because it is one of the over-represented pathways (Supplementary Table 2). A recent study illustrated the role of miR-144 in regulating the progression of non-alcoholic steatohepatitis in high-fat-diet induced metabolic syndrome E3 rats [25]. Interestingly, neuron related pathways were found to be enriched in the pathways that miR-146a/146b is involved in (Supplementary table 2), which indicated that the neuron systems in adipose tissues were also activated during cold exposure. Although further experimental work is needed, our pathway analysis predicts that adipose-neuron cross-talk occurs in the cold stimulation of adipose tissues. Taken together, although miR-144 and miR-146a-5p altered their expression levels in cold-induced adipose tissue, their role in BAT development should be illustrated by a more detailed mechanism.

MiRNAs exert their function through target genes. We searched the literature and selected two putative targets (Phlda1 and Bmpr1b) for miR-144-3p, one (Sphk2) for miR-146a-5p for further validation. Our data revealed the opposite expression pattern of miR-144-3p and Phlda1 in both BAT and WAT, which suggesting miR-144-3p might play the function in BAT activation through Phlda1. It has been illustrated that Phlda1 gene is critical in energy homeostasis [22], mice model of miR-144-3p will be a good tool to validate the target interaction of miR-144-3p and Phlda1 *in vivo*. Another potential target, Bmpr1b, a type 1 receptor in the TGFβ pathway, was found to be expressed oppositely with miR-144-3p in BAT specifically (Fig. 4A and C). The reason might be that miR-144-3p regulates Bmpr1b at post-transcriptional level in WAT. However, recent study showed that Bmpr1b knockout didn't affect the BAT weight [23], its function in adaptive thermogenesis, and interaction with miR-144-3p still need to be deeply investigated. Sphk2 (a potential target of miR-144-3p), a member of the sphingosine kinase family, has been shown to regulate adipogenesis and insulin resistance [27,28]. Again, the opposite expression pattern of miR-146a and Sphk2 were only found specific in BAT (Fig. 4B and D). To fully evaluate their interaction in adipose tissue remodeling,

further studies will require the generation of mouse models with adipose-specific ablation of the miRNA or/and gene.

In addition, our studies identified three DE miRNAs, miR-3060-5p, miR-5126 and miR-3960, that exhibited the dramatic up-regulation (fold change 33.94, 14.1 and 6.85, respectively) in cold-stimulated BAT (Table 1). Very limited information about these miRNAs can be found from a literature search. Our data suggest that they are involved in cold-induced BAT activation, and further studies will be needed to explore the detailed mechanism.

In summary, our study provides robust evidence of miRNA response in cold-induced BAT activation and Ing-WAT browning and highlights the information that is of relevance for understanding the mechanisms related to thermogenic adipose tissue. Further functional studies on detailed miRNA-mRNA interactions may provide new insights into the effects of miRNA on BAT activation.

Conflict of interest

All authors declare that there are no conflicts of interest.

Acknowledgments

This work was supported by the State Key Development Program for Basic Research of China (NO. 2015CB943100), the National Swine Industry Technology System (NO. CARS-36-10B), the National Natural Science Foundation of China (NO. 31330074 and 31172189) and the Agricultural Science and Technology Innovation Program (No. ASTIP-IAS-TS-02).

Appendix A. Supplementary data

Supplementary data related to this article can be found at http://dx.doi.org/10.1016/j.bbrc.2015.05.014.

Transparency document

Transparency document related to this article can be found online at http://dx.doi.org/10.1016/j.bbrc.2015.05.014.

References

[1] J. Wu, P. Boström, L.M. Sparks, L. Ye, J.H. Choi, A.-H. Giang, et al., Beige adipocytes are a distinct type of thermogenic fat cell in mouse and human, Cell 150 (2012) 366–376.
[2] K.A. Virtanen, M.E. Lidell, J. Orava, M. Heglind, R. Westergren, T. Niemi, et al., Functional brown adipose tissue in healthy adults, N. Engl. J. Med. 360 (2009) 1518–1525.
[3] M. Rosell, M. Kaforou, A. Frontini, A. Okolo, Y.-W. Chan, E. Nikolopoulou, et al., Brown and white adipose tissues: intrinsic differences in gene expression and response to cold exposure in mice, Am. J. Physiol. Endocrinol. Metab. 306 (2014) E945–E964.
[4] Q. Hao, R. Yadav, A.L. Basse, S. Petersen, S.B. Sonne, S. Rasmussen, et al., Transcriptome profiling of brown adipose tissue during cold exposure reveals extensive regulation of glucose metabolism, Am. J. Physiol. Endocrinol. Metab. 308 (2014) E380–E392.
[5] H. Ohno, K. Shinoda, B.M. Spiegelman, S. Kajimura, PPAR agonists induce a white-to-brown fat conversion through stabilization of PRDM16 protein, Cell Metab. 15 (2012) 395–404.
[6] T.B. Waldén, I.R. Hansen, J.A. Timmons, B. Cannon, J. Nedergaard, Recruited vs. nonrecruited molecular signatures of brown, "brite," and white adipose tissues, Am. J. Physiol. Endocrinol. Metab. 302 (2012) E19–E31.
[7] M. Rosenwald, A. Perdikari, T. Rülicke, C. Wolfrum, Bi-directional interconversion of brite and white adipocytes, Nat. Cell Biol. 15 (2013) 659–667.
[8] M. Trajkovski, H. Lodish, MicroRNA networks regulate development of brown adipocytes, Trends Endocrinol. Metab. 24 (2013) 442–450.
[9] P. Arner, A. Kulyté, MicroRNA regulatory networks in human adipose tissue and obesity, Nat. Rev. Endocrinol. 11 (2015) 276–288.
[10] R. Mudhasani, V. Puri, K. Hoover, M.P. Czech, A.N. Imbalzano, S.N. Jones, Dicer is required for the formation of white but not brown adipose tissue, J. Cell. Physiol. 226 (2011) 1399–1406.
[11] H.-J. Kim, H. Cho, R. Alexander, H.C. Patterson, M. Gu, K.A. Lo, et al., MicroRNAs are required for the feature maintenance and differentiation of brown adipocytes, Diabetes 63 (2014) 4045–4056.
[12] M. Trajkovski, K. Ahmed, C.C. Esau, M. Stoffel, MyomiR-133 regulates brown fat differentiation through Prdm16, Nat. Cell Biol. 14 (2012) 1330–1335.
[13] Y. Chen, F. Siegel, S. Kipschull, B. Haas, H. Fröhlich, G. Meister, et al., miR-155 regulates differentiation of brown and beige adipocytes via a bistable circuit, Nat. Commun. 4 (2013) 1769.
[14] M. Mori, H. Nakagami, G. Rodriguez-Araujo, K. Nimura, Y. Kaneda, Essential role for miR-196a in brown adipogenesis of white fat progenitor cells, PLoS Biol. 10 (2012) e1001314.
[15] R.K. Patel, M. Jain, NGS QC Toolkit: a toolkit for quality control of next generation sequencing data, PloS One 7 (2012) e30619.
[16] R. Nogales-Cadenas, P. Carmona-Saez, M. Vazquez, C. Vicente, X. Yang, F. Tirado, et al., GeneCodis: interpreting gene lists through enrichment analysis and integration of diverse biological information, Nucleic Acids Res. 37 (2009) W317–W322.
[17] W. Zhao, Y. Mu, L. Ma, C. Wang, Z. Tang, S. Yang, et al., Systematic identification and characterization of long intergenic non-coding RNAs in fetal porcine skeletal muscle development, Sci. Rep. 5 (2015) 8957.
[18] S. Zhao, J. Zhang, X. Hou, L. Zan, N. Wang, Z. Tang, et al., OLFML3 expression is decreased during prenatal muscle development and regulated by MicroRNA-155 in pigs, Int. J. Biol. Sci. 8 (2012) 459–469.
[19] Z.-Z. Zhao, L.-L. Xin, J.-H. Xia, S.-L. Yang, Y.-X. Chen, K. Li, Long-term high-fat high-sucrose diet promotes enlarged islets and β-cell damage by oxidative stress in Bama Minipigs, Pancreas (2015).
[20] M. Fasshauer, J. Klein, K.M. Kriauciunas, K. Ueki, M. Benito, C.R. Kahn, Essential role of insulin receptor substrate 1 in differentiation of brown adipocytes, Mol. Cell. Biol. 21 (2001) 319–329.
[21] M. Baranowski, A. Blachnio-Zabielska, T. Hirnle, D. Harasiuk, K. Matlak, M. Knapp, et al., Myocardium of type 2 diabetic and obese patients is characterized by alterations in sphingolipid metabolic enzymes but not by accumulation of ceramide, J. Lipid Res. 51 (2010) 74–80.
[22] S. Basseri, S. Lhoták, M.D. Fullerton, R. Palanivel, H. Jiang, E.G. Lynn, et al., Loss of TDAG51 results in mature-onset obesity, hepatic steatosis, and insulin resistance by regulating lipogenesis, Diabetes 62 (2013) 158–169.
[23] T.J. Schulz, P. Huang, T.L. Huang, R. Xue, L.E. McDougall, K.L. Townsend, et al., Brown-fat paucity due to impaired BMP signalling induces compensatory browning of white fat, Nature 495 (2013) 379–383.
[24] L. Sun, H. Xie, M.A. Mori, R. Alexander, B. Yuan, S.M. Hattangadi, et al., Mir193b-365 is essential for brown fat differentiation, Nat. Cell Biol. 13 (2011) 958–965.
[25] D. Li, X. Wang, X. Lan, Y. Li, L. Liu, J. Yi, et al., Down-regulation of miR-144 elicits proinflammatory cytokine production by targeting toll-like receptor 2 in nonalcoholic steatohepatitis of high-fat-diet-induced metabolic syndrome E3 rats, Mol. Cell. Endocrinol. 402 (2015) 1–12.
[26] M. Balasubramanyam, S. Aravind, K. Gokulakrishnan, P. Prabu, C. Sathishkumar, H. Ranjani, et al., Impaired miR-146a expression links subclinical inflammation and insulin resistance in type 2 diabetes, Mol. Cell. Biochem. 351 (2011) 197–205.
[27] T. Hashimoto, J. Igarashi, H. Kosaka, Sphingosine kinase is induced in mouse 3T3-L1 cells and promotes adipogenesis, J. Lipid Res. 50 (2009) 602–610.
[28] L. Dai, Y. Qi, J. Chen, D. Kaczorowski, W. Di, W. Wang, et al., Sphingosine kinase (SphK) 1 and SphK2 play equivalent roles in mediating insulin's mitogenic action, Mol. Endocrinol. 28 (2014) 197–207. Baltim. Md.